4D Lung Imaging with Time-resolved 3D MRI and low Pitch helical CT: Comparison of two Techniques for the Assessment of Tumour Size and Displacement in a ventilated ex-vivo Set up

J. Biederer[1,2], J. Dinkel[3], G. Remmert[3], H. Bolte[4], T. Welzel[5], M. Fabel[3], C. Thierfelder[6], M. Bock[3], J. Debus[5], M. Heller[4], and H-U. Kauczor[3]

[1]Department of Diagnostic Radiology, University Hospital Schleswig-Holstein, Campus Kiel, Kiel, Schleswig-Holstein, Germany, [2]Radiology, German Cancer Research Center, Heidelberg, Baden-Württemberg, Germany, [3]German Cancer Research Center, [4]University Hospital Schleswig-Holstein Campus Kiel, [5]University Hospital Heidelberg, [6]Siemens Medical Systems, Forchheim, Germany

Introduction: Motion-adapted radiotherapy with gated irradiation or tracking of tumour positions requires dedicated 4D imaging techniques for selection of patients and treatment planning. The objective was to compare the concepts of MRI with dynamic 3D-GRE acquisitions and 4D-imaging with retrospectively reconstructed low pitch helical CT. Tumour size and displacement during respiration were evaluated in an ex-vivo system.

Materials and Methods: We used an MR-compatible chest phantom for porcine heart-lung preparations with a flexible silicone reconstruction of a diaphragm [1]. The rhythmic in- and deflation of the diaphragm with water (1.5 L) induced a displacement of lung tissue resembling diaphragmatic breathing. The phantom walls were filled with 1.25g/L $NiSO_4$. Three lungs were prepared with 12 artificial nodules (30g/L agarose, 0.125 mM/L Gd-DTPA (Magnevist, Schering, Berlin, Germany) and 1.5g/L iodine (5mL Ultravist 300, Schering, Berlin, Germany); mean nodule volume 0.86 mL (range 0.50-1.21mL; SD 0.22mL); mean diameters 1.51x1.04x1.45 cm³, mean nodule density on CT 80+/-20 HU). 1,5 T MRI were obtained with a 6 channel phased array body coil (Magnetom Symphony, Siemens, Erlangen, Germany, G_{max}=30 mT/m). Images during ventilation (8/min) and at static conditions were obtained with a dynamic 3D-GRE sequence with temporal interpolation (TREAT in coronal orientation; TR=2.13ms, TE=0.72ms, □=10°, BW=810Hz/px, 48 partitions, FOV 350mm, matrix 128x102, TA=53s, temporal res. 2.1s/image, voxel size 3.4x2.7x3.8mm³ [2]). 40-row detector CT images were acquired during respiration (8/min) and at fixed inspiration (collimation 24x1.2 mm, pitch 0.1, rotation time 1s, slice 1.5 mm, increment 0.8mm, effective temporal resolution 500ms) [3]. MR data sets coincident with 0/25/50/75/100% inspiration and equivalent recontructions from dynamic and static 4D CT scans were evaluated by 3 independent observers. Transverse (largest "x" and perpendicular to this "y") and axial diameters ("z") were measured with the distance tool of a commercial workstation (Leonardo, Siemens, Erlangen, Germany). Nodule displacement along the z-axis was measured on coronal image reformations (fig. 1). The variation coefficient (VC) was used as indicator for the reproducibility of measurements (interobserver-VC for different observers; interphase-VC for measurement by the same observers but in different respiratory phases; interscan-VC for the same observers, but from different acquisitions in the same respiratory phase (MRI only)). Statistical significance was tested with Wilcoxon matched pairs test (p<0.05 for the level of significance). As internal standard, we used automatic computer-aided lung nodule volumetry from CT (LungCare, Siemens, Forchheim, Germany) [4].
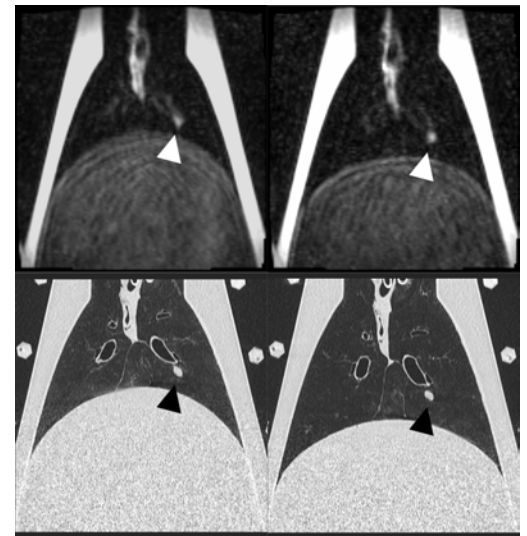

Fig. 1: Porcine lung inflated inside the artificial chest. Coronal images from the 3D GRE series (above) and 4D CT (below) representing ex- (left) and inspiration (right). The arrowheads indicate an artificial nodule close to the left main bronchus.

n = 12 nodules	Distance [cm]; (SD [cm])		Interobserver-VC [%]; (SD [%])		Interphase-VC [%]; (SD [%])		Interscan-VC [%]; (SD [%])	
Parameter	MRI	CT	MRI	CT	MRI	CT	MRI	CT
x static	1,65 [0.25]	1.51 [0.24]	6.65 [3.83]	1.34 [0.76]	n. a.	n. a.	3.08 [1.63]	n. a.
x dynamic	1,67 [0.25]	1.54 [0.24]	6.37 [2.74]	2.71 [1.24]	7.77 [3.4]	2.57 [0.99]	6.42 [3.13]	n. a.
y static	1.19 [0.18]	1.04 [0.18]	9.30 [4.42]	2.52 [1.72]	n. a.	n. a.	5.46 [3.57]	n. a.
y dynamic	1.24 [0.17]	1.07 [0.18]	7.45 [3.21]	5.09 [3.13]	9.80 [4.90]	4.01 [2.62]	8.45 [4.66]	n. a.
z static	1.53 [0.36]	1.45 [0.39]	6.04 [2.80]	2.45 [3.35]	n. a.	n. a.	3.67 [1.38]	n. a.
z dynamic	1.64 [0.34]	1.51 [0.41]	6.90 [3.72]	4.72 [2.87]	10.36 [4.18]	3.86 [1.91]	7.49 [4.98]	n. a.
Displacement static	1.39 [0.56]	1.88 [0.73]	9.90 [8.11]	1.96 [2.49]	n. a.	n. a.	n. a.	n. a.
Displacement dynamic	n.a.	1.6 [0.69]	n.a.	0.57 [1.48]	n. a.	n. a.	n. a.	n. a.

Results: The experiment provided a realistic simulation of respiratory motion. Maximum displacement at the top of the diaphragm (2.7 cm-3.6 cm, mean 3.2 cm) was in the same range as observed during tidal breathing in human patients. Lesion diameters from MRI were 5.5-15.9% larger than with CT (tab.). Instead, maximum nodule displacement from ex- to inspiration was approximately 24% lower on MRI. Both effects are explained by the lower temporal resolution of MRI which leads to apparent enlargement of nodules and underestimation of extreme positions at minima and maxima of the respiratory curve. Interobserver-VC for diameters from 4D MRI were 2.2-6.8% higher than from CT (p<0.001). Interphase-VC for different CT reconstructions and MRI obtained at different respiratory phases differed in the same range (p<0.001). Due to motion effects, interscan-VC from dynamic MRI was significantly lower compared to static scans (3.08-5.46% vs. 6.42-8.45%, p<0.001). Computer-aided volumetry from CT as the internal standard was characterized by a low interobserver-VC (0.58%/1.04% for static/ dynamic). Mean volumes from static/dynamic CT (0.86 mL vs. 0.86 mL; p=0.81) and interphase-VC for volumetry did not differ (3.05% vs. 3.29%, p=0.06).

Discussion: Reproducibility for measurements of nodule size and displacement from 4D-MRI was better than expected. The ex-vivo experience suggested that 4D-MRI might be suitable for the evaluation of patients who are considered to be elective for motion-adapted therapy. The principal advantage of 4D-MRI over 4D-CT is its capability of repeated acquisitions at different respiratory conditions without additional radiation exposure. However, spatial and temporal resolution are inferior to CT. Furthermore, MR does not provide X-ray attenuations for radiotherapy planning. Taking into account that measurement errors in three lesion diameters multiply, computer aided volumetry of CT scans showed by far the best reproducibility. To transfer this concept to MRI would improve the reproducibility of lesion measurements on 4D-MRI. It also remains subject to further investigation, how faster acquisition times will reduce motion-related errors. In particular parallel imaging techniques and new acquisition schemes are expected to improve the performance of dynamic 3D MRI of the lung opening the perspective to make it a useful tool for analysing respiration dynamics on a routine base.

References: 1) Biederer J, Plathow C, Schoebinger M, Tetzlaff R, Puderbach M, Bolte H, Zaporozhan J, Meinzer HP, Heller M, Kauczor HU. Reproducible Simulation of Respiratory Motion in Porcine Lung Explants. Fortschr Röntgenstr 2006; 178: 1067-1072; 2) Korosec FR, Frayne R, Grist TM, Mistretta CA. Time-resolved contrast-enhanced 3D MR angiography. Magn Reson Med 1996;36:345-351; 3) Mageras GS, Yorke E. Deep inspiration breath hold and respiratory gating strategies for reducing organ motion in radiation treatment. Semin Radiat Oncol 2004;14:65-75; 4) Bolte H, Riedel C, Jahnke T, Inan N, Freitag S, Kohl G, Heller M, Biederer J. Reproducibility of computer-aided volumetry of artificial small pulmonary nodules in ex vivo porcine lungs. Invest Radiol 2006;41:28-35